



2,3',4,4',5'-Pentamethoxy-*trans*-stilbene, a resveratrol derivative, is a potent inducer of apoptosis in colon cancer cells via targeting microtubules

Haitao Li^a, William Ka Kei Wu^{b,c}, Zongping Zheng^a, Chun Tao Che^{d,1}, Le Yu^b, Zhi Jie Li^b, Ya Chun Wu^b, Ka-Wing Cheng^a, Jun Yu^{c,1}, Chi Hin Cho^{b,e,*}, Mingfu Wang^{a,**}

^a School of Biological Sciences, The University of Hong Kong, Pokfulam Road, Hong Kong, China

^b School of Biomedical Sciences, The Chinese University of Hong Kong, Hong Kong, China

^c Department of Medicine and Therapeutics, The Chinese University of Hong Kong, Hong Kong, China

^d School of Chinese Medicine, The Chinese University of Hong Kong, Hong Kong, China

^e Institute of Digestive Diseases, The Chinese University of Hong Kong, Hong Kong, China

ARTICLE INFO

Article history:

Received 20 May 2009

Accepted 30 June 2009

Keywords:

Resveratrol
Polymethoxystilbene
Colon cancer
Microtubule
Apoptosis

ABSTRACT

Resveratrol, a naturally occurring polyphenolic antioxidant, is a compound holding promise for cancer chemoprevention. Previous studies suggest that 2,3',4,5'-tetramethoxy-*trans*-stilbene (TMS) and 3,4,4',5'-tetramethoxy-*trans*-stilbene (MR-4), both of which are derivatives of resveratrol, are potent apoptosis-inducing agents with clinical potential. In this study, we chemically synthesized 2,3',4,4',5'-pentamethoxy-*trans*-stilbene (PMS), the hybrid molecule of TMS and MR-4, and determined its effects on colon cancer growth. When compared with its parent compounds, PMS displayed more potent *in vitro* anti-mitogenic effect on colon cancer cells (Caco-2, HT-29 and SW1116). Moreover, PMS inhibited tumor growth *in vivo* in a colon cancer xenograft model. In this connection, PMS strongly induced apoptosis in HT-29 cells as evidenced by increased PARP cleavage, DNA fragmentation, and accumulation of sub-G₁ population. Further mechanistic analysis revealed that PMS enhanced the polymerization of microtubules, which was followed by G₂/M mitotic arrest and caspase-dependent apoptosis. The activation of caspases-3, -7, -8, and -9 was involved in PMS-induced apoptosis with concomitant down-regulation of the pro-survival PI3K/Akt signaling. Collectively, these data suggest that PMS is a potent inducer of apoptosis via targeting microtubules and may merit investigation as a potential chemoprophylactic and therapeutic agent for colon cancer.

© 2009 Elsevier Inc. All rights reserved.

1. Introduction

Colorectal cancer, the third most frequent non-cutaneous malignancy, was also the third leading cause of cancer-related death in United States [1]. Despite the recent improvements in preventive strategies, screening techniques and development of chemotherapy, the median overall survival period for patients with

metastatic colorectal cancer is only 24 months. Moreover, the optimal method for early detection is controversial and patient compliance with screening recommendations remains a major hurdle to overcome. Resistance to current chemotherapeutic drugs also represents an important clinical issue in which attempt to treat patients simultaneously with different classes of therapeutics has yielded some success by reducing its development. At the cellular level, evasion of apoptosis represents a common molecular pathway for carcinogenesis and drug resistance [2]. The development of novel apoptosis-inducing agents therefore becomes greatly in need and represents an important challenge in medicinal chemistry.

There are three major approaches in drug discovery: empiric screening, rational design of new compounds, and chemical modification of known molecules with established pharmacological actions. During the course of identifying compounds active for the prevention and treatment of cancer, resveratrol (3,4',5-trihydroxy-*trans*-stilbene) and its derivatives have emerged to hold promise for their potent *in vitro* and *in vivo* anticancer bioactivities [3]. Resveratrol belongs to a class of chemical known as stilbenes which exhibit variable antioxidant, anti-inflammatory

Abbreviations: PI3K, phosphatidylinositol 3-kinase; Akt, protein kinase B; MAPK, mitogen-activated protein kinase; Erk, extracellular signal-regulated kinase; p38, p38 mitogen-activated protein kinases; JNK, c-Jun amino-terminal kinase; U0126, 1,4-diamino-2,3-dicyano-1,4-bis(o-aminophenylmercapto)butadiene ethanolate; SB203580, 4-(4-fluorophenyl)-2-(4-methylsulfinylphenyl)-5-(4-pyridyl)-1H-imidazole; SP600125, 1,9-pyrazoloanthrone anthrapyrazolone.

* Corresponding author at: School of Biomedical Sciences, The Chinese University of Hong Kong, Hong Kong, China. Tel.: +852 2696 6886; fax: +852 2603 5139.

** Corresponding author at: School of Biological Sciences, The University of Hong Kong, Hong Kong, China. Tel.: +852 2299 0338; fax: +852 2299 0340.

E-mail addresses: chcho@cuhk.edu.hk (C.H. Cho), mfwang@hkusua.hku.hk (M. Wang).

¹ Both the authors contributed a lot to flow cytometry and *in vivo* study, considering the possible interest conflict.

and apoptosis-inducing properties mainly based on the substituents on the stilbene skeleton. In general, the number and position of the hydroxyl groups on the benzene rings determine their radical-scavenging activity and selective inhibitory activity on cyclooxygenase-2, while methoxyl groups are mainly related to their apoptosis-inducing activity [4–6].

In relation to the current development of resveratrol derivatives as anticancer agents, methoxylated stilbenes have been emerging as a novel class of apoptosis-inducing agents, among which 3,4,4',5-tetramethoxy-*trans*-stilbene (MR-4) and 2,3',4,5'-tetramethoxy-*trans*-stilbene (TMS) have attracted much attention due to their potent pro-apoptotic activities [7–15]. MR-4 is currently under preclinical evaluation as a potential anticancer drug for colorectal cancer chemotherapy while TMS displays substantial inhibitory effect on the proliferation of cultured breast cancer cells and the growth of cancer xenograft by induction of apoptosis. For methoxylated stilbenes, previous structure–activity relationship analysis revealed that 3,5-dimethoxy and 3,4,5-trimethoxy motifs are important to the pro-apoptotic activity while 2-methoxyl group in the stilbene skeleton confers selectivity against cancer cells by targeting cytochrome P450 CYP1B1, a tumor-specific enzyme whose expression is only detected in cancer but not normal tissues. In light of these facts, we presumed that 2,3',4,4',5'-pentamethoxy-*trans*-stilbene (PMS), a hybrid molecule of MR-4 and TMS, may be a more potent and selective apoptosis-inducing agent than their parent compounds. In this study, we would describe the synthesis of PMS and its biological activity and mechanism of action on colon cancer.

2. Materials and methods

2.1. Reagents and chemicals

Methoxylated stilbenes were chemically synthesized by the classic Wittig couplings from the corresponding methoxylated diethyl benzylphosphonate and suitable methoxylated benzylbromide [4,5] (see [Supplementary Materials](#)). Caspase inhibitors (Z-VAD-FMK, Z-DEVE-FMK, Z-IETD-FMK and Z-LEHD-FMK) were obtained from EMD Chemicals, Inc. (San Diego, CA, USA). All other chemicals were obtained from Sigma–Aldrich (St Louis, MO, USA) unless otherwise specified. All primary antibodies were purchased from Cell Signaling Technology (Beverly, MA, USA). Stock solutions of tested compounds were prepared in dimethyl sulfoxide (DMSO), stored at -20°C and protected from the light.

2.2. Cell culture and viability assay

The human colon cancer cells Caco-2, HT-29 and SW1116 were obtained from the American Type Culture Collection (Manassas, VA, USA) and maintained in RPMI 1640 (Invitrogen, Carlsbad, CA, USA) containing 10% fetal bovine serum (Invitrogen), 100 U/mL penicillin G, 100 $\mu\text{g}/\text{mL}$ streptomycin, and maintained at 37°C , 95% humidity, and 5% carbon dioxide. Necrotic cell death was determined by lactate dehydrogenase release assay (Roche, Indianapolis, IN, USA).

2.3. Cell proliferation assay

Cell proliferation was measured by MTT [3-(4,5-dimethylthiazol-2-yl)-2,5-diphenyltetrazolium bromide] assay. Cells were plated at a density of 6000 cells per well in 96-well plates. After treatment, MTT solution dissolved in the culture medium at the final concentration of 0.5 mmol/L was added to each well and the plates were incubated for another 4 h. DMSO was then added to solubilize MTT tetrazolium crystal. Finally, the optical density was determined at 570 nm using a Benchmark Plus microplate reader

(Bio-Rad, Hercules, USA). Morphological analysis was performed by phase contrast light microscopy and documented by the digital camera system (Nikon TS100, Nikon, Tokyo, Japan). The IC_{50} values were calculated from the linear portion of dose–response curves.

2.4. DNA ladder formation

In brief, HT-29 cells (5×10^5) were plated per well on six-well plates and allowed to incubate overnight for attachment, and then they were treated as indicated. After treatment, cells were collected and their DNA was extracted using a Wizard[®]SV genomic DNA purification system kit (Promega, Madison, WI, USA) as recommended by the manufacturer. After electrophoresis on 1.7% agarose gel, the DNA samples (1 $\mu\text{g}/\text{lane}$) were visualized by Gel-Red[™] staining (Biotium Inc., Hayward, CA, USA) under UV illumination.

2.5. Quantitation of nucleosomes by ELISA

Briefly, 1×10^4 HT-29 cells per well in 100 μL medium were seeded onto 96-well plates. After 24-h, the cells were treated as indicated. To quantitate the effects of drug treatment on apoptosis, a nucleosome ELISA kit (Roche Diagnostics Corporation, Indianapolis, IL, USA) was used to quantitate the enrichment of histone-associated DNA fragments which were released into the cytoplasm according to the procedure provided by the manufacturer. The amount of nucleosomes was expressed as the absorbance value.

2.6. Flow cytometry analysis

In brief, 5×10^5 HT-29 cells were plated per well on 6-well plates and incubated for 24 h for attachment, then were treated with either PMS (20 μM) or DMSO (0.1%, *v/v*) for 12, 24, 36 or 48 h. After treatment, cells were fixed with ice-cold 70% ethanol in phosphate buffered saline followed by incubation with 50 $\mu\text{g}/\text{mL}$ propidium iodide, 3.8 mmol/L sodium citrate, 10 $\mu\text{g}/\text{mL}$ RNase A at 4°C for 3 h and analyzed by flow cytometry (Beckman Coulter Epics XL-MCL, UK). The cell cycle phase distribution and proportion of apoptotic cells (% of sub- G_1 phase) were calculated from the resultant DNA histogram using Multicycle AV version 3.0 software (Phoenix Flow System, San Diego, CA, USA).

2.7. Confocal immunofluorescence analysis

HT-29 cells were seeded onto Petri dishes with glass bottoms and allowed to incubate for 24 h for attachment, after which cells were treated with PMS (20 μM) or DMSO (0.1%, *v/v*) for 24, 48 or 72 h. At the end of incubation, cells were fixed with 4% (*v/v*) paraformaldehyde for 30 min and then made permeable with methanol at -20°C for 10 min. The cells were then covered with 10% (*v/v*) goat serum for 30 min at room temperature to block non-specific adsorption of antibodies to the cells. After this procedure, the cells were incubated with primary antibody against α -tubulin at 4°C overnight. Cells were then probed with Alexa Fluor 488 goat anti-rabbit secondary antibodies and incubated at room temperature for another 2 h. Fluorescent signals were detected using a confocal fluorescence microscope (Nikon EZ-C1, Nikon, Tokyo, Japan).

2.8. Tubulin polymerization assay

The tubulin polymerization was determined using a tubulin polymerization assay kit (BK004, Cytoskeleton Inc., Denver, CO, USA) as described by the manufacturer. Briefly, half area 96-well plates were warmed to 37°C for 30 min prior to starting the assay. 1 mL general tubulin buffer (GTB: 80 mM Pipes, pH 6.9, 2 mM MgCl_2 , and 0.5 mM EGTA) was warmed to room temperature for

drug dilutions. Purified bovine tubulin (4 mg) was re-suspended with 1 mL cold (4 °C) PEM plus 10% glycerol buffer on ice for 3 min. After 10 μ L of general tubulin buffer, 2 mM taxol stock and PMS stocks were added into each well and incubated for 2 min at 37 °C, 100 μ L reconstituted tubulin above was added directly to the testing wells followed by reading with a SpectraMax 250 (Global Medical Instrumentation Inc., Ramsey, MN, USA) in kinetic mode, 61 cycles of 1 reading per cycle at 340 nm with 5 s medium orbital shaking.

2.9. Western blot

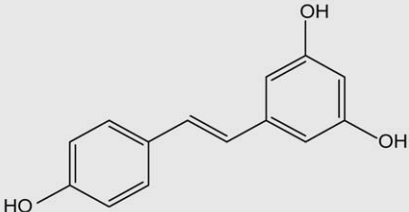
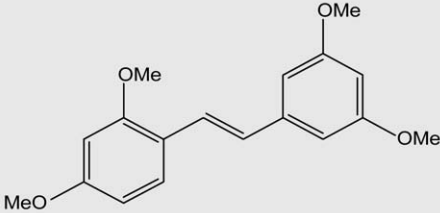
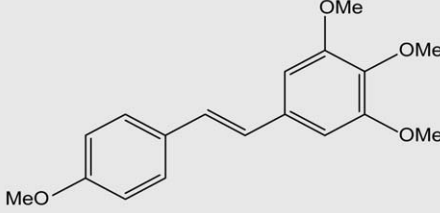
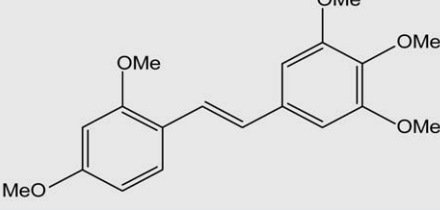
Briefly, 1.5×10^5 HT-29 cells per well in 2 mL medium were seeded onto 6-well plates and incubated for 24 h. After treatment, the cells were lysed in radioimmunoprecipitation assay buffer [50 mmol/L Tris-HCl (pH 7.5), 150 mmol/L sodium chloride, 0.5% a-cholate acid, 0.1% SDS, 2 mmol/L EDTA, 1% Triton X-100, and 10% glycerol], containing 1.0 mmol/L phenylmethylsulfonyl fluoride and 1 μ g/mL aprotinin. After sonication for 30 s on ice and centrifuging for 20 min at $12,000 \times g$ at 4 °C, the supernatant was collected and total protein concentration was determined by a standard Bradford assay reagent (Bio-Rad) using bovine serum albumin as standard.

Cell lysates were stored at –20 °C. 20 μ g of protein samples were resolved on SDS-PAGE and transferred to Hybond C nitrocellulose membranes (Amersham Corporation, Arlington Heights, IL, USA). The membranes were probed with primary antibodies dissolved in wash buffer containing 5% non-fat milk powder overnight at 4 °C and incubated for 1 h with secondary antibodies conjugated with peroxidase (1:2000). Chemiluminescent signals were then developed with Lumiglo reagent (Cell Signaling Technology, Beverly, MA, USA) and detected and quantified by the ChemiDoc XRS gel documentation system (Bio-Rad, Hercules, CA, USA).

2.10. Nude mice xenograft model

To evaluate the direct inhibitory action of PMS on cancer growth *in vivo*, a HT-29 colon cancer xenograft model was adopted. In brief, HT-29 colon cancer cells were trypsinized, collected and re-suspended in phosphate buffered saline (2×10^7 cells/mL). Cell viability was confirmed to be above 95% based on trypan blue staining. Then 3×10^6 HT-29 cells in 0.2 mL phosphate buffered saline were injected subcutaneously into the right flank or dorsal region of 4–6-week-old female BALB/c nu/nu mice. After inoculation,

Table 1
Effect of resveratrol and its derivatives on cell proliferation.

Tested compounds	Chemical structure	IC ₅₀ (μ M)		
		In Caco-2	In HT-29	In SW1116
Resveratrol		127.7 \pm 25.0	152.1 \pm 17.6	88.3 \pm 10.0
TMS		>100	24.9 \pm 5.2	37.0 \pm 6.7
MR-4		32.1 \pm 3.7	20.0 \pm 5.8	>100
PMS		65.5 \pm 7.3	14.7 \pm 4.4	27.2 \pm 8.9

Human colon adenocarcinoma cells (Caco-2, HT-29 and SW1116) were treated with tested compounds at different concentrations for 48 h. Then, cell proliferation was evaluated by MTT assay, and IC₅₀ was determined from a plot of inhibitory percent versus logarithm of concentration. Data are presented as mean \pm SEM of three independent experiments.

the mice were maintained under sterile condition and the size of tumor formed was measured using calipers every 3 days. Tumor volume (V) was estimated according the following formula: tumor volume (V) = $L \times W^2/2$, where L is the mid-axis length and W is the mid-axis width. After the tumors reached a mean size of 130 mm³ (on day 10), PMS (25, 100 mg/kg) dissolved in 5% (v/v) DMSO/olive oil was given to the nude mice every other day for 24 days. Animals in control group received 5% (v/v) DMSO/olive oil, respectively. All treatments were administered by intraperitoneal injections in mice at 0.1 mL per 10 g of body weight. At the end of the experiment, the mice were sacrificed and tumors were excised for further assays.

2.11. Statistical analysis

All cell line experiments were performed at least three times independently. Statistical analysis was done by using the prism statistical package (GraphPad Software, San Diego, CA, USA). Turkey's t -test was used to compare data between two groups. One-way ANOVA and the Bonferroni correction were used to compare data between three and more groups. Values were expressed as means \pm SEM. $P < 0.05$ was considered statistically significant.

3. Results

3.1. The effect of PMS on colon cancer cell growth

Initially, the cytotoxicity of stilbenes was investigated in several human colon cancer cells including Caco-2, HT-29 and SW1116 by MTT assay. The IC₅₀ values of tested compounds were computed

based on the data collected from at least three times respective assays. As shown in Table 1, PMS displayed much more potent cytotoxic effect on colon cancer cells than resveratrol. And PMS was about 10-fold more potent than resveratrol in inhibiting the HT-29 cell growth. Notably, compared with TMS and MR-4, PMS exhibited effective growth inhibitory effect against all three tested colon cancer lines. In terms of potency and spectrum, PMS was superior to its parent compounds TMS and MR-4, and may merit investigation as a potential chemoprophylactic and therapeutic agent for colon cancer. Considering HT-29 was much more sensitive than Caco-2 and SW1116 in response to PMS treatment, HT-29 cell line was selected for subsequent mechanistic study and treated by PMS at 20 μ M/L, at which inhibits 50–75% cell growth.

3.2. Absence of significant necrotic toxicity

To understand the mechanism of PMS to inhibit the colon cancer growth, the generalized necrotic toxicity was examined and excluded firstly. Generally, in normal live cells and apoptotic cells the integrity of the cell membrane is maintained, while in necrotic cells the integrity of plasma membrane was lost and resulted in the release of cytoplasmic enzymes such as lactate dehydrogenase. As shown in Supplementary Fig. 1A, there is little necrotic cell death taken place after PMS treatment even at 30 μ M. Clearly, necrosis is not the main cause for the cytotoxicity of PMS.

3.3. PMS induces apoptosis in colon cancer cells

We noticed that after PMS treatment for 48 h, the majority of cells detached the bottom of the culture wells, floated in the

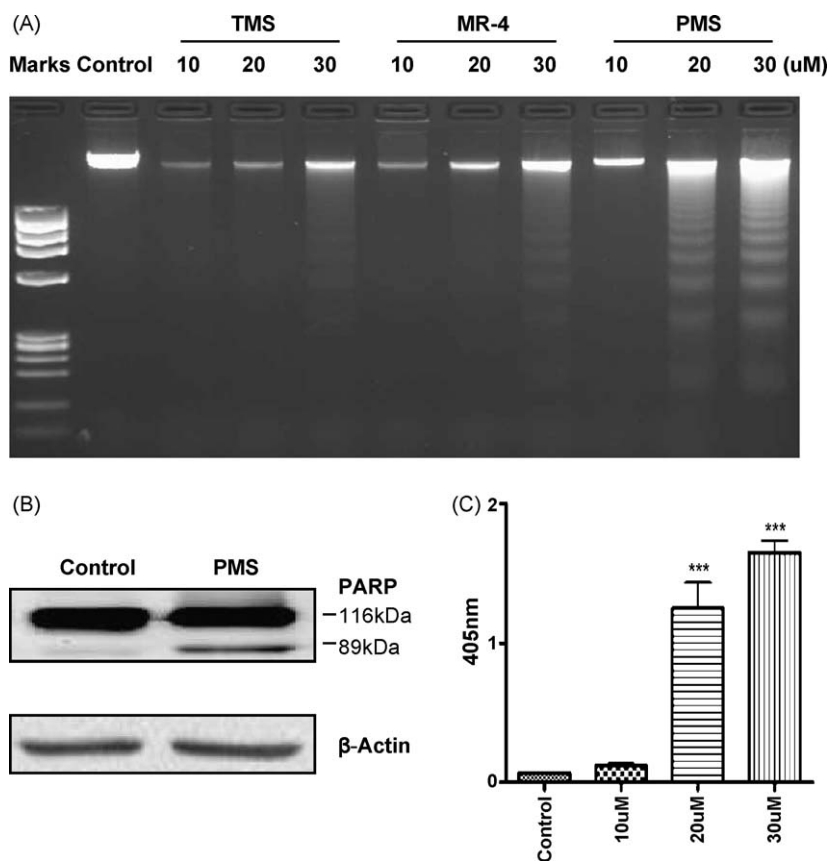


Fig. 1. PMS induces apoptotic cell death in human colon adenocarcinoma HT-29 cells. (A) After PMS treatment at 20 μ M for 48 h, DNA ladder formation was observed in HT-29 cells. (B) After PMS treatment at 20 μ M for 48 h, the effect of PMS on the PARP cleavage was examined by Western blot. (C) After PMS treatment for 48 h, the enrichment of cytoplasmic nucleosomes in treated HT-29 cell was substantially enhanced in a dose-dependent manner. Data are presented as mean \pm SEM ($n = 3$) of a representative experiment performed in triplicate. *** $p < 0.001$ versus respective control group.

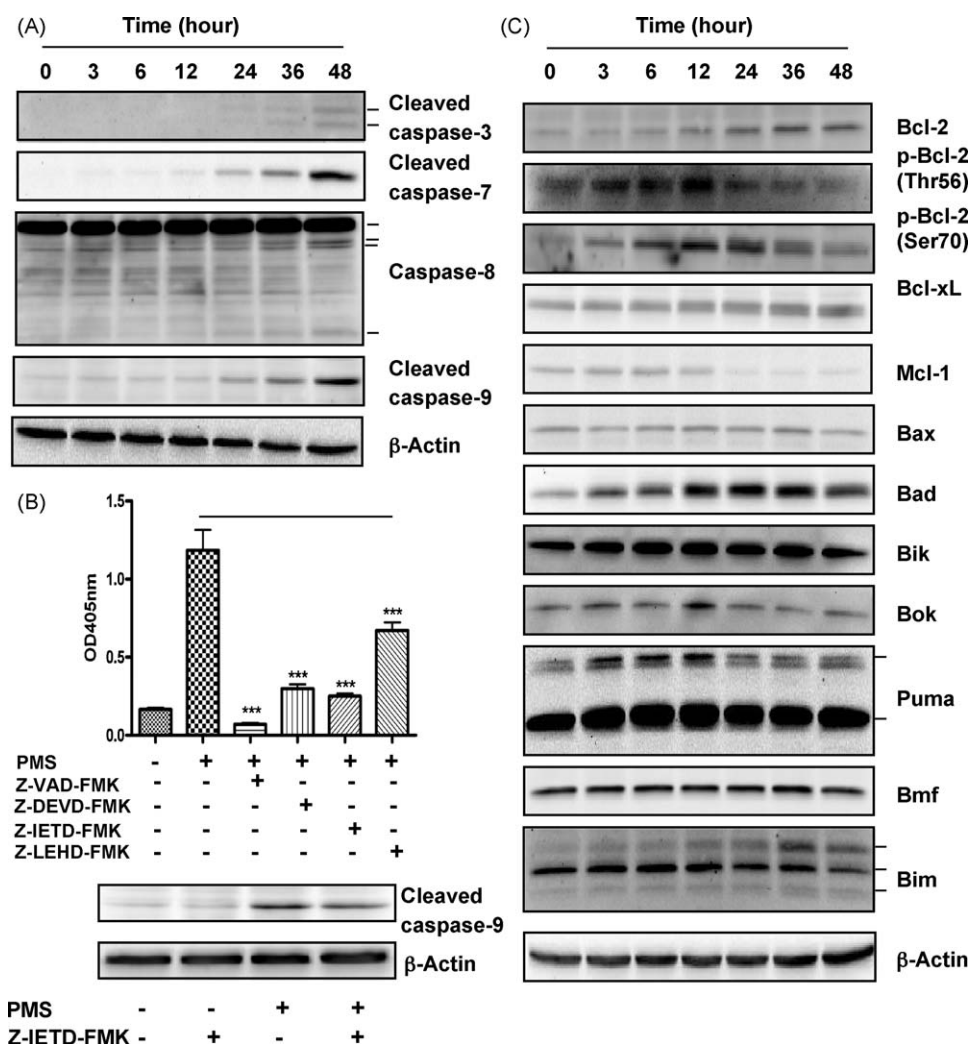


Fig. 2. Effects of PMS on caspase activation and Bcl-2 family expression. (A) Caspases involved in PMS-induced apoptosis were identified by Western blot. (B) The functional relevance of caspase-3, -8 and -9 activation during PMS-induced apoptosis was evaluated using their specific inhibitors (20 μ M, pretreatment for 1 h before 20 μ M PMS treatment) by a nucleosome ELISA kit (ELISA^{PLUS} kit, Roche). *** p < 0.001 versus PMS-treated group. (C) The effect of PMS on expression of Bcl-2 family was examined by Western blot. After incubation with PMS at 20 μ M for 3, 6, 12, 24, 36, 48 h, HT-29 cells were lysed and protein was extracted for Western blot analysis.

medium and exhibited apoptosis-like morphological characteristics such as nuclear condensation and segmentation, suggesting the possibility of apoptosis. To verify this hypothesis, the classical hallmarks and molecular signature of apoptosis such as DNA ladder formation and the cleavage of Poly (ADP-ribose) polymerase (PARP) were therefore examined (Fig. 1A and B). After 48 h PMS treatment, both DNA ladder formation and the increase of PARP cleavage were observed in HT-29. Notably, from the lowest concentration needed to induce DNA ladder formation in HT-29, PMS was found to be a more potent apoptosis-inducing agent than its parent compounds, TMS and MR-4.

To better quantitatively determinate apoptosis induced by PMS, a Cell Death Detection ELISA^{PLUS} kit from Roche was used to detect mono- and oligonucleosomes which are released into the cytoplasm in undergoing apoptosis cells. As shown in Fig. 1C, PMS treatment significantly increased the double-strand DNA and nucleosomes released into the cytoplasm. After PMS treatment at 20 μ M for 48 h the enrichment of double-strand DNA and nucleosomes in cytoplasm was 20 times higher than control. Meanwhile, apoptotic effect of PMS was also confirmed in Caco-2 cells (Supplementary Fig. 1B).

3.4. Molecular mechanisms of apoptosis induced by PMS in HT-29 cells

3.4.1. Caspase activation

Although coordinated activation of caspases plays a central role in the execution of most types of apoptosis, there is now accumulating evidence supporting that apoptosis can occur in caspase-independent manner [16–18]. For this reason, v-VAD-FMK, the pan-caspase inhibitor, was used to examine whether caspase activation involve PMS-induced apoptosis or not. The nearly complete blockage of PMS-induced apoptosis by pretreatment with v-VAD strongly indicated that PMS induced apoptosis in caspase-dependent manner. Accordingly, caspases involved in PMS-induced apoptosis were identified by Western blot. As shown in Fig. 2A, the cleavage of procaspase-3, -8 and -9 and the formation of corresponding active forms were observed. To further evaluate the functional relevance of caspase-3, -8 and -9 activation during PMS-induced apoptosis, several caspase specific inhibitors were used. As shown in Fig. 2B, pretreatment of HT-29 cells with caspase-3, -8 and -9 inhibitors for 1 h significantly decreased PMS-induced apoptotic DNA fragment formation by 74.7%, 78.7% and 43.2%, respectively.

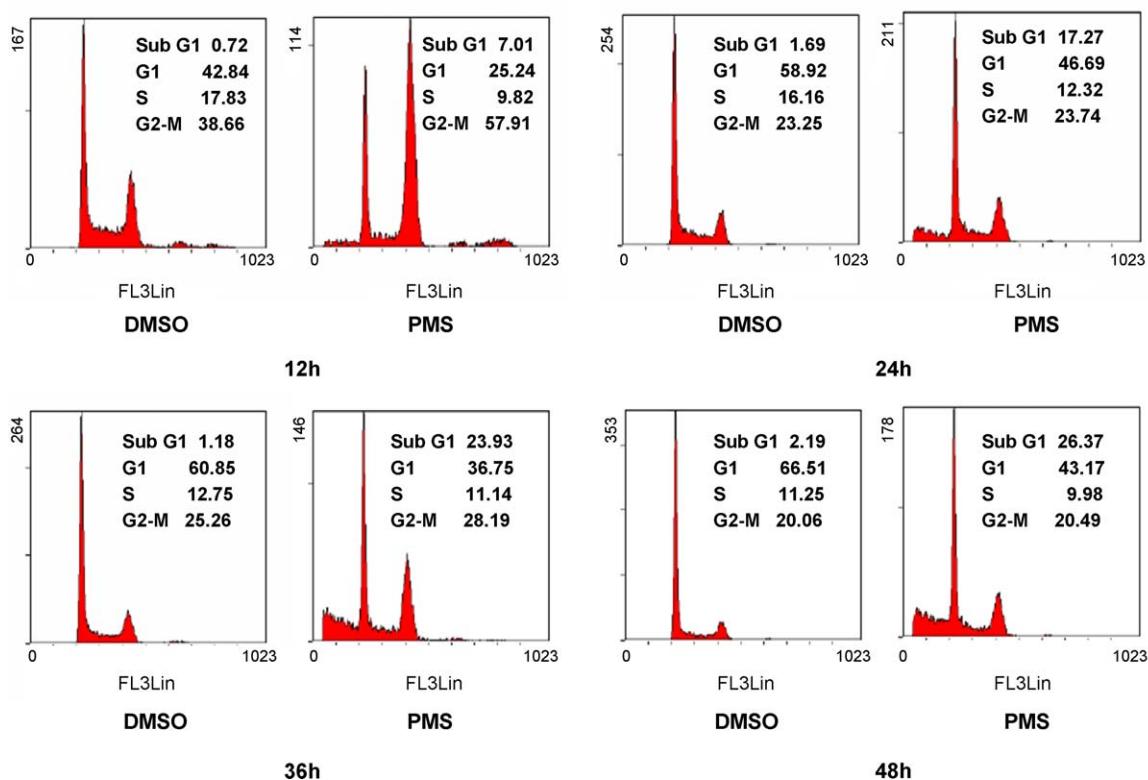


Fig. 3. Effect of PMS on cell cycle distribution. After incubation with DMSO (0.1%, *v/v*) or PMS at 20 μ M for 12, 24, 36 and 48 h, HT-29 cells were collected, stained by propidium iodide and subjected to flow cytometry for cell cycle analysis.

3.4.2. Bcl-2 family proteins

The regulation of caspase activation and the consequent apoptotic cell death relies on an intricate balance of the expression of pro- and anti-apoptotic members of Bcl-2 family [19]. For the pro-apoptotic members, up-regulation of Bad, Bik, Bok, Bim and α -Puma was observed after PMS treatment and the expression was peaked at 12-h, while the expression levels of Bax and Bmf were kept relatively constant (Fig. 2C). As to the anti-apoptotic members, we observed that Mcl-1 expression was down-regulated while Bcl-xL remained stable. Surprisingly, Bcl-2 protein expression and its phosphorylation at both Thr56 and Ser70 residues were substantially up-regulated by PMS treatment. The phosphorylation of Bcl-2 increased substantially within the initial 12 h after PMS treatment and gradually decreased afterward. It is noted that such multi-site Bcl-2 phosphorylation (also called hyper phosphorylation) often occurs in apoptosis induced by microtubule-interfering agents and results in inhibition of Bcl-2's anti-apoptotic function [20].

3.5. PMS induced G₂/M cell cycle arrest

All those findings above indicated that the potent inhibitory effect of PMS on HT-29 cell growth may be mainly contributed to the apoptotic cell death. To examine the hypothesis above, HT-29 cells were treated with PMS at 20 μ M for 48 h in the presence of pan-caspase inhibitor (Z-VAD-FMK) at 10 μ M, a concentration at which Z-VAD-FMK completely abolished the occurrence of apoptotic cell death induced by PMS. Nevertheless, pretreatment of Z-VAD-FMK failed to protect HT-29 cells against the cytotoxic effect of PMS (Supplementary Fig. 2A). As LDH activity in the culture medium was not affected by caspase inhibitor pretreatment, those cells above were analyzed by flow cytometry and found that there is a substantial accumulation at the G₂/M-phase (Supplementary Fig. 2B and C). Accordingly, effect of PMS on cell

cycle distribution and apoptosis was examined. 12-h treatment of PMS induced a substantial accumulation of HT-29 cells at the G₂/M-phase which was followed by apoptosis as indicated by a time-dependent increase of cells in the sub-G₁ phase (Fig. 3). Taken together, these results provide evidence for a key role of G₂/M phase cell cycle arrest playing in the anti-proliferative effect of PMS.

3.6. PMS interfered with mitosis and enhanced microtubule polymerization

G₂/M cell cycle arrest and timely associated Bcl-2 hyperphosphorylation were extensively reported to occur in apoptosis induced by microtubule-interfering agents [21–23]. Considering the similar chemical structure of PMS to combrestatin, a famous anticancer drug targeting microtubules, we hypothesized that PMS might also interfere with microtubule polymerization.

To test the hypothesis above, microtubule organization and mitosis in response to PMS treatment were initially examined by immunofluorescent microscopy. After PMS treatment, the cells were poorly spread and the microtubule became short and stubby (Fig. 4Ac). As in apoptosis induced by microtubule targeting drugs [14,21], highly abnormal mitotic spindles and multinucleated cells were also observed in PMS-treated cells (Fig. 4Ad, e and f). The effect of PMS on microtubule polymerization was further confirmed by tubulin polymerization assay (Fig. 4B). Results showed that PMS enhanced tubulin polymerization in a dose-dependent manner and exhibited comparable microtubule-stabilizing effect to paclitaxel.

3.7. PMS inhibits tumor growth in vivo

The direct anticancer activity of PMS *in vivo* was evaluated using a 24-day colon cancer xenograft model in nude mice. After incubation of cancer cells 10 days, tumors reached a mean size of

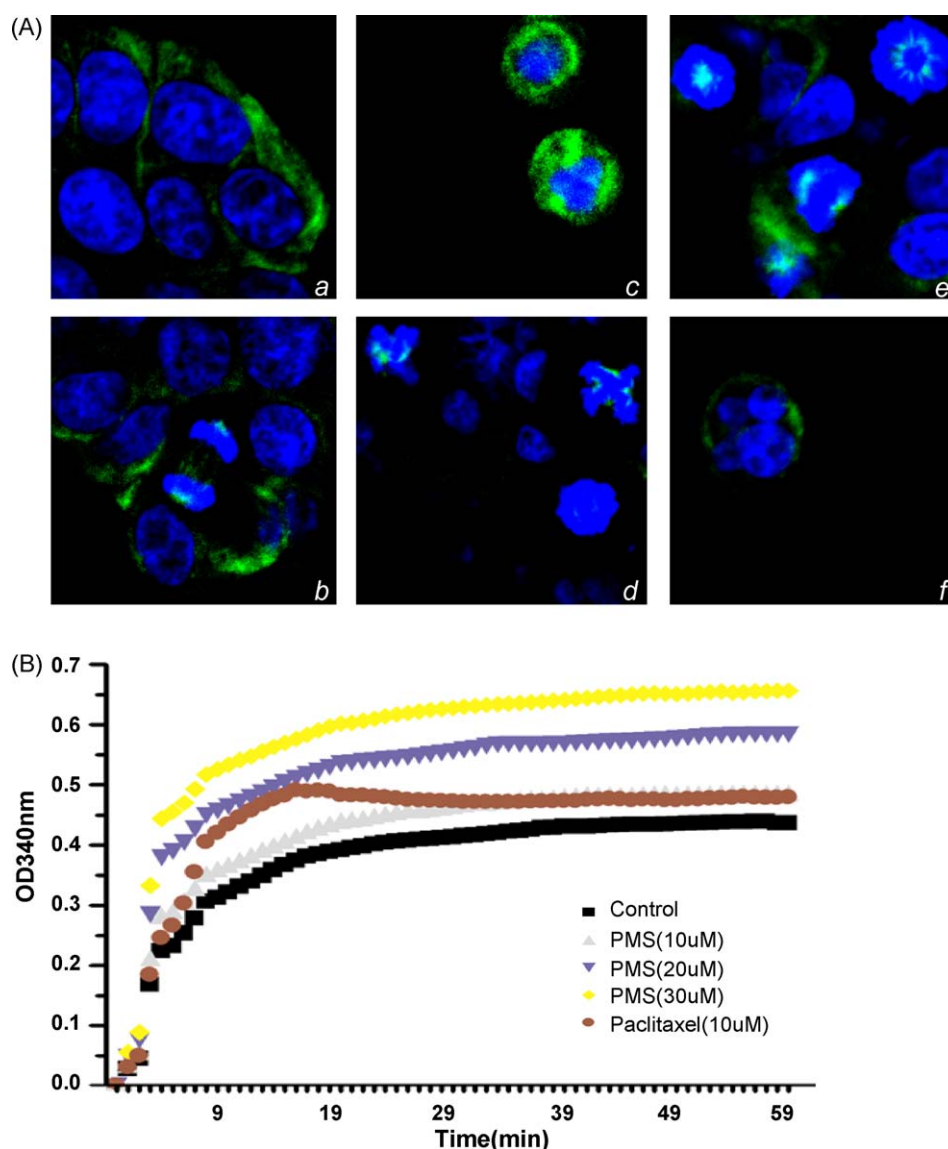


Fig. 4. Effect of PMS on mitosis and microtubule polymerization. (A) After PMS treatment for 48 h, the effect of PMS on microtubule organization *in vitro* was examined by confocal immunofluorescence images. (Aa and Ab) Control cells; (Ac, Ad, Ae and Af) PMS at 15 μ M for 72 h. Original magnification: 400 \times . (B) PMS enhanced tubulin polymerization in a concentration-dependent manner. Tubulin polymerization assay was carried out using a CytoDYNAMIX Screen 01 kit. Polymerization was started by incubating purified tubulin with different concentration PMS at 37 $^{\circ}$ C, and absorption readings at 340 nm were monitored for 60 min.

150 mm³. Animals were grouped and treated as mentioned in materials and methods. 24 days of continuous PMS treatment (25, 100 mg/kg body weight, intraperitoneal injection) significantly reduced the tumor volume by 31% and 39%, respectively (Fig. 5A). Moreover, based on the data about body weight (Fig. 5B), visible inspection of general appearance and organs histology, PMS was well tolerated in mice, and no obvious systemic toxicity was observed during the entire period of drug treatment.

4. Discussion

In this study, we verified the hypothesis PMS, a hybrid molecule from the TMS and MR-4, is a promising apoptosis-inducing agent for colorectal cancer chemotherapy. Based on the data collected in this study and those of others, we hypothesized signal pathway of targeted compound: the interaction of PMS with microtubules results in microtubule damage which is detected by G₂/M checkpoint, leads to the persistent G₂/M cell cycle arrest, and subsequently trigger the molecular signaling for the following caspase-dependent apoptosis. Despite the potent inhibitory effect

on colon cancer cell proliferation *in vitro*, our *in vivo* data suggests that PMS only exerted moderate antitumor activity when used as a single chemotherapeutic agent. It is known that the development of polymethoxylated stilbenes as therapeutic agents have been limited by their poor water-solubility. To improve such pharmacological properties, further rational design is needed, and the introduction of the phosphate ester moiety or the boronic acid group is suggested.

There are two distinct but interconnected pathways, namely, death receptor- and mitochondria-mediated pathways in the regulation of apoptosis. In the present study, we found that PMS-induced apoptosis was in caspase-dependent manner and the inhibition of caspase-9 and caspase-8 reduces PMS-induced apoptosis by 43.2% and 78.7%, respectively. This finding may reflect the scenario that caspase-8, the mediator of death receptor pathway, is the predominant transducer of PMS-induced apoptosis and part of the pro-apoptotic signaling of caspase-8 is mediated through caspase-9. Although our findings suggest that caspase-8 may be a predominant transducer of PMS-induced apoptosis, the expression of either p43/p41 or p18 fragment of caspase-8 was

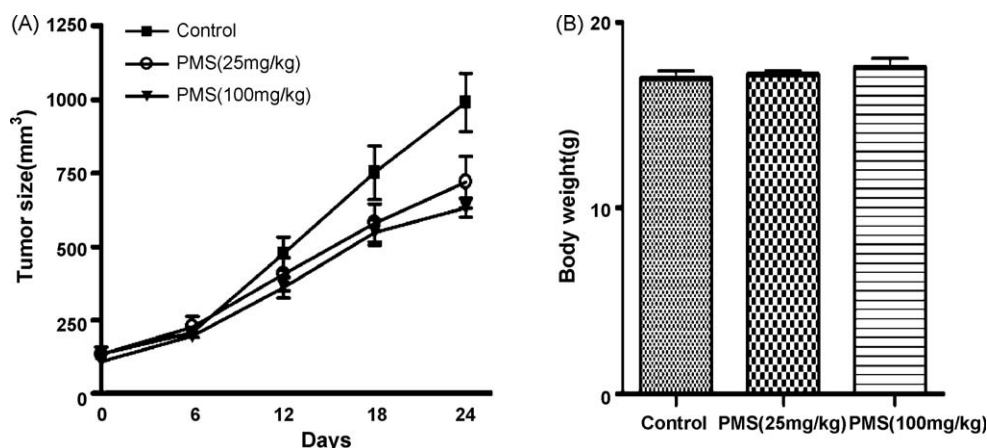


Fig. 5. The study on anticancer activity of PMS *in vivo* using HT-29 colon cancer cells xenograft model in nude mice. Intraperitoneal injection of PMS (25, 100 mg/kg body weight) on alternate days for a total of 24 days significantly reduced (A) the tumor volume by 31% ($p < 0.05$ versus control group) and 39% ($p < 0.05$ versus control group) without affecting (B) body weight. 3×10^6 HT-29 cells in 0.2 mL phosphate buffered saline were injected subcutaneously into the right flank or dorsal region of 4–6-week-old female BALB/c nu/nu mice. After the tumors reached a mean size of 130 mm³ (on day 10), PMS dissolved in 5% (v/v) DMSO/olive oil was given to the nude mice every other day for 24 days. Animals in control group received 5% (v/v) DMSO/olive oil, respectively. The size of tumor formed was measured using calipers every other day. Data are presented as mean \pm SEM ($n = 8$).

very weak. It is possible that there is an insufficient amount of active caspase-8 or downstream caspases in the early stage of apoptosis, and caspase-8 amplifies the apoptotic signaling by caspase-8-Bid-mitochondrial pathway. Consistent with the hypothesis above, PMS-induced caspase-9 activation was significantly reduced but not blocked completely by pretreatment with caspase-8 inhibitor (Fig. 2B), suggesting the direct activation of caspase-9 without caspase-8 involvement. In this respect, down-regulation of Akt phosphorylation has been reported to induce overexpression of total Bad which ultimately activates caspase-9 and the effector caspase(s), rendering the cells more susceptible to the apoptotic signaling [24]. To this end, our results indicate that PMS substantially reduced Akt phosphorylation as early as 6 h after treatment (Supplementary Fig. 3A), and such down-regulation of Akt phosphorylation is paralleled by the up-regulation of total Bad.

PMS triggers G₂/M phase cell cycle arrest and Bcl-2 hyperphosphorylation, prompting us to speculate that microtubule is the direct target of PMS. It is to note that pan-caspase inhibitor (Z-VAD-FMK) pretreatment, although inhibiting the apoptotic cell death completely, failed to prevent cell growth inhibition induced by PMS treatment, suggesting that the persistent mitotic arrest at G₂/M phase can play an important role in anti-proliferative activity of PMS. In this case, the following apoptotic event seems to be a secondary event of such mitotic block.

Treating cancer cells with microtubule-interfering agents is generally associated with G₂/M cell cycle arrest followed by apoptosis. To improve the basic knowledge of MIA-induced cell death, we also tried to find the potential links between PMS-induced mitotic arrest and apoptosis, but the definitive mechanisms involved remained unknown. Currently, there are many studies indicated that Bcl-2 and/or Bcl-xL hyperphosphorylation by CDC2 or JNK, Bad phosphorylation on serine 128 by CDK1 and Bim activation by JNK may be the potential mediators linking MIAs-induced mitotic arrest and apoptosis [22,25–30]. However, our data clearly indicated that MAPKs (ERK, p38, and JNK) did not play a critical role in the PMS-induced apoptotic response as pharmacological inhibition of MAPKs did not affect cytotoxicity as well as pro-apoptotic activity of PMS (Supplementary Fig. 3A and B). Moreover, considering the key role of apoptosis signaling pathway *via* direct activation of executioner caspase-3 and -7 by caspase-8, the major mechanism linking such mitotic arrest and apoptosis in this study is unknown because those proposed mechanism above only enable to explain the initiating event in the mitochondrial pathway of apoptosis. Our results are in

agreement with previous reports demonstrating that caspase-8 activation independent of cell death receptor has been observed in microtubule-interfering agents treated cells [31,32]. To improve our understanding on the relationship between PMS-induced mitotic block and caspase-8 activation will be the next challenging task in future.

As cytoskeletal components, the importance of microtubules in the process of mitosis makes them the promising targets for anticancer drug. Actually, microtubules may be the best cancer target to be identified so far, and several microtubule targeting agents have been ranked the most successful clinical cancer chemotherapeutic drugs currently. As to the most potent cytotoxic stilbene derivatives, most of them, especially those possessing a trimethoxybenzene ring, were found to be microtubule-targeting agents [13–15,33]. In our study, PMS also exhibited potent anticancer activity *in vivo* without obvious systemic toxicity during whole period of drug treatment. Considering neurotoxicity is the principle side effect of clinical microtubule-interfering agents, the data in this field is greatly needed [23,34]. Although such anti-microtubule drugs have been used in the clinic for many years, the cause of the neurotoxicity is poorly understood, but undoubtedly involves the effects of the drugs on microtubules which are the key component of neurons. As no neurotoxicity data were collected in this study, it is unknown whether with the administration of PMS, peripheral neuropathy and reversible myelosuppression caused or not, so further study in these areas is required.

Acknowledgments

The authors thank Dr. Qicai Liu and Ms. Wing Ki Cheung for technical help in performing tubulin polymerization assay and flow cytometry analysis.

Appendix A. Supplementary data

Supplementary data associated with this article can be found, in the online version, at [doi:10.1016/j.bcp.2009.06.109](https://doi.org/10.1016/j.bcp.2009.06.109).

References

- [1] Jemal A, Siegel R, Ward E, Hao Y, Xu J, Murray T, et al. Cancer statistics. *CA Cancer J Clin* 2008;58:71–96.

- [2] Hanahan D, Weinberg RA. The hallmarks of cancer. *Cell* 2000;100:57–70.
- [3] Jang M, Cai L, Udeani GO, Slowing KV, Thomas CF, Beecher CW, et al. Cancer chemopreventive activity of resveratrol, a natural product derived from grapes. *Science* 1997;275:218–20.
- [4] Wang M, Jin Y, Ho CT. Evaluation of resveratrol derivatives as potential antioxidants and identification of a reaction product of resveratrol and 2,2-diphenyl-1-picrylhydrazyl radical. *J Agric Food Chem* 1999;47:3974–7.
- [5] Murias M, Handler N, Erker T, Pleban K, Ecker G, Saiko P, et al. Resveratrol analogues as selective cyclooxygenase-2 inhibitors: synthesis and structure-activity relationship. *Bioorg Med Chem* 2004;12:5571–8.
- [6] Murias M, Jager W, Handler N, Erker T, Horvath Z, Szekeres T, et al. Antioxidant, prooxidant and cytotoxic activity of hydroxylated resveratrol analogues: structure-activity relationship. *Biochem Pharmacol* 2005;69:903–12.
- [7] Kim S, Ko H, Park JE, Jung S, Lee SK, Chun YJ. Design, synthesis, and discovery of novel trans-stilbene analogues as potent and selective human cytochrome P450 1B1 inhibitors. *J Med Chem* 2002;45:160–4.
- [8] Robeti M, Pizziranti D, Simoni D, Rondanin R, Baruchello R, Bonora C, et al. Synthesis and biological evaluation of resveratrol and analogues as apoptosis-inducing agents. *J Med Chem* 2003;46:3546–54.
- [9] Sale S, Verschoyle RD, Boocock D, Jones DJL, Wilsher N, Rupareliak C, et al. Pharmacokinetics in mice and growth-inhibitory properties of the putative cancer chemopreventive agent resveratrol and the synthetic analogue trans 3,4,5,4'-tetramethoxystilbene. *Br J Cancer* 2004;90:736–44.
- [10] Sale S, Tunstall RG, Potter GA, Steward WP, Gescher AJ. Comparison of the effects of the chemopreventive agent resveratrol and its synthetic analog trans 3,4,5,4'-tetramethoxystilbene (DMU212) on adenoma development in the *Apc^{Min}* mouse and cyclooxygenase-2 in human-derived colon cancer cells. *Int J Cancer* 2005;115:194–201.
- [11] Gossiau A, Chen M, Ho CT, Chen KY. A methoxy derivative of resveratrol analogue selectively induced activation of mitochondrial apoptotic pathway in transformed fibroblasts. *Br J Cancer* 2005;92:513–21.
- [12] Lion CJ, Matthews CS, Stevens MFG, Westwell AD. Synthesis, antitumor evaluation, and apoptosis-inducing activity of hydroxylated (*E*)-stilbenes. *J Med Chem* 2005;48:1292–5.
- [13] Simoni D, Romagnoli R, Baruchello R, Rondanin R, Rizzi M, Pavani MG, et al. Novel combretastatin analogues endowed with antitumor activity. *J Med Chem* 2006;49:3143–52.
- [14] Park H, Aiyar SE, Fan P, Wang J, Yue W, Okouneva T, et al. Effects of tetramethoxystilbene on hormone-resistant breast cancer cells: biological and biochemical mechanisms of action. *Cancer Res* 2007;67:5717–26.
- [15] Ma Z, Molavi O, Haddadi A, Lai R, Gossage RA, Lavasanifar A. Resveratrol analog trans 3,4,5,4'-tetramethoxystilbene (DMU-212) mediates anti-tumor effects via mechanism different from that of resveratrol. *Cancer Chemother Pharmacol* 2008;63:27–35.
- [16] Shi Y. Mechanisms of caspase activation and inhibition during apoptosis. *Mol Cell* 2002;9:459–70.
- [17] Degterev A, Boyce M, Yan J. A decade of caspases. *Oncogene* 2003;22:8543–67.
- [18] Kroemer G, Martin SJ. Caspase-independent cell death. *Nat Med* 2005;11:725–30.
- [19] Kuwana T, Newmeyer DD. Bcl-2-family proteins and the role of mitochondria in apoptosis. *Curr Opin Cell Biol* 2003;15:691–9.
- [20] Ruvoilo PP, Deng X, May WS. Phosphorylation of Bcl-2 and regulation of apoptosis. *Leukemia* 2001;15:515–22.
- [21] Srivastava RK, Srivastava AR, Korsmeyer SJ, Nesterova M, Cho-Chung YS, Longo DL. Involvement of microtubules in the regulation of Bcl-2 phosphorylation and apoptosis through cyclic AMP-dependent protein kinase. *Mol Cell Biol* 1998;18:3509–17.
- [22] Furukawa Y, Iwase S, Kikuchi J, Terui Y, Nakamura M, Yamada H, et al. Phosphorylation of Bcl-2 protein by CDC2 kinase during G2/M phases and its role in cell cycle regulation. *J Biol Chem* 2000;275:21661–7.
- [23] Mollinedo F, Gajate C. Microtubules, microtubule-interfering agents and apoptosis. *Apoptosis* 2003;8:413–50.
- [24] Datta SR, Ranger AM, Lin MZ, Sturgill JF, Ma YC, Cowan CW, et al. Survival factor-mediated BAD phosphorylation raises the mitochondrial threshold for apoptosis. *Dev Cell* 2002;3:631–43.
- [25] Pumiglia KM, Decker SJ. Cell cycle arrest mediated by the MEK/mitogen-activated protein kinase pathway. *Proc Natl Acad Sci USA* 1997;94:448–52.
- [26] McDaid HM, Horwitz SB. Selective potentiation of paclitaxel(taxol)-induced cell death by mitogen-activated protein kinase inhibition in human cancer cell lines. *Mol Pharmacol* 2001;60:290–301.
- [27] Fan M, Goodwin M, Vu T, Brantley FC, Gaarde WA, Chambers TC. Vinblastine-induced phosphorylation of Bcl-2 and Bcl-xL is mediated by JNK and occurs in parallel with inactivation of the Raf-1/MEK/ERK cascade. *J Biol Chem* 2000;275:29980–5.
- [28] Konishi Y, Lehtinen M, Donovan N, Bonni A. Cdc2 phosphorylation of BAD links the cell cycle to the cell death machinery. *Mol Cell* 2002;9:1005–16.
- [29] Tseng CJ, Wang YJ, Liang YC, Jeng JH, Lee WS, Lin JK, et al. Microtubule damaging agents induced apoptosis in HL60 cells and G2/M cell cycle arrest in HT-29 cells. *Toxicology* 2002;175:123–42.
- [30] Lei K, Davis RJ. JNK phosphorylation of Bim-related members of the Bcl2 family induces Bax-dependent apoptosis. *Proc Natl Acad Sci USA* 2003;100:2432–7.
- [31] Goncalves A, Braguer D, Carles G, Andre N, Prevot C, Briand C. Caspase-8 activation independent of CD95/CD95-L interaction during paclitaxel-induced apoptosis in human colon cancer (HT29-D4). *Biochem Pharmacol* 2000;60:1579–84.
- [32] Haefen CV, Wieder T, Essmann F, Schulze OK, Dorken B, Daniel PT. Paclitaxel-induced apoptosis in BJAB cells proceeds via a death receptor-independent, caspase-3/-8-driven mitochondrial amplification loop. *Oncogene* 2003;22:2236–47.
- [33] Cushman M, Nagarathnam D, Gopal D, He HM, Lin CM, Hamel E. Synthesis and evaluation of analogues of (Z)-1-(4-methoxyphenyl)-2-(3,4,5-trimethoxyphenyl) ethene as potential cytotoxic and antimetabolic agents. *J Med Chem* 1992;35:2293–306.
- [34] Jordan MA, Wilson L. Microtubules as a target for anticancer drugs. *Nat Rev Cancer* 2004;4:253–65.